

Amorphous and micromorph Si solar cells: current status and outlook

Vitaliy AVRUTIN*, Natalia IZYUMSKAYA, Hadis MORKOÇ

Department of Electrical and Computer Engineering, Virginia Commonwealth University, Richmond, VA, USA

Received: 24.06.2014 • Accepted: 11.09.2014 • Published Online: 10.11.2014 • Printed: 28.11.2014

Abstract: An overview of the current status and prospects of thin-film Si photovoltaics, including both hydrogenated amorphous and microcrystalline Si as well their combination known as micromorph solar cells, with a major focus on the technological development is given. Although thin-film Si solar cells have been one of the first commercially successful photovoltaic devices, today they face a tremendous challenge from variety of bulk Si technologies (mono- and multicrystalline Si) and compound-semiconductor thin-film solar cells, both of which have managed to substantially reduce the production cost and improve power conversion efficiency. Thin-film Si photovoltaics benefiting from the mighty mainstream Si industry have demonstrated the ability to reduce the production cost and cost per peak power; however, the performance improvement of amorphous-Si panels has been only marginal and further progress is hard to expect. The power conversion efficiencies of micromorph solar cells have already exceeded those of amorphous-Si devices. However, to improve their market penetration and even to hold their current share, the micromorph Si solar modules need to improve their performance, which today is approaching 11%, along the path to potential 15%, while keeping the manufacturing cost low. Further progress will require the improvement of light-trapping technologies and contact performance.

Key words: Photovoltaics, amorphous silicon solar cells, micromorph, amorphous silicon, microcrystalline silicon

1. Introduction

In recent years, the photovoltaics (PV) market has steadily grown at a rate of 30% per year or higher. The production of solar-cell modules has reached 35 GW in 2013. The demand has increased by 35% (or 9 GW of power) in the first quarter of 2014 compared to the previous year first-quarter record. For the entire year 2014, the forecast is to exceed 50 GW [1]. Further rapid growth of PV industry is expected over the next 5 years, with up to 100 GW annual deployment being targeted in 2018, according to the latest forecast released by NPD Solarbuzz Marketbuzz [2].

Despite the tremendous efforts focused on the search for and development of new PV technologies, almost the entire production of PV modules is represented by the so-called first- and second-generation solar cells (SCs). The first-generation photovoltaics include a variety of technologies based on bulk Si wafers, including both large-grain polycrystalline (also dubbed as multicrystalline) and single-crystalline Si. The second-generation photovoltaics are represented in the market by 3 thin-film technologies, which encompass cadmium telluride (CdTe), copper indium diselenide/copper indium-gallium diselenide variety (CuInSe₂ or CIS and Cu(InGa)Se₂ or CIGS), and silicon thin-film variety (hydrogenated amorphous Si, a:Si:H, and microcrystalline Si, μ c-Si:H

*Correspondence: vavrutin@vcu.edu

(also known as “nanocrystalline”) as well as their a-Si:H/ μ c-Si:H combination (known as micromorph solar cells).

Currently the market is dominated by bulk Si PV modules comprising about 90% of all the PV modules shipped in 2013 [3]. The fastest growth is observed in the segment of multicrystalline Si panels, which increased their share from slightly over 50% in 2010 to 62% at the time of writing. Although the production of thin-film PV modules also grew, their share fell from 15% to about 10%. Out of the 3 dominating thin-film technologies (CdTe, a-Si/ μ m-Si, CIS/CIGS), only the CIS/CIGS-based solar cells increased their share (see Figure 1) compared to 2010 [3]. However, it would not be accurate to state that thin-film photovoltaics are in decline. Thin-film solar cells offer some advantages over the mainstream bulk-Si photovoltaics. Although thin-film solar cells are currently less efficient than their bulk-silicon counterparts, they have a low temperature coefficient for output power due to a larger bandgap. As a result, thin-film solar cells generate greater power in geographic regions where temperature is high. Furthermore, this technology drastically reduces the use of semiconductor materials by depositing a thin layer (typically a few micrometers) of a semiconductor material over a sheet of metal or glass. In addition, they are lighter, an important feature to be considered. As a result, the thin-film technologies provide the lowest price per peak watt, although the rapidly declining prices of multicrystalline-Si panels are making it increasingly difficult for them to compete in the rooftop market. Currently the lowest price in the PV industry is 0.49 \$/Wp for CdTe modules produced by First Solar Ltd. [4]. Thin-film Si have been proven to also offer very competitive prices (in the range around 0.5 \$/Wp [5]), benefiting from the mainstream Si technology; however, to improve the market penetration or even hold its current market share, this technology needs to improve module performance towards crystalline technology and competing thin-films technologies exhibiting rapid progress in the power conversion efficiency. The power conversion efficiencies of CdTe modules

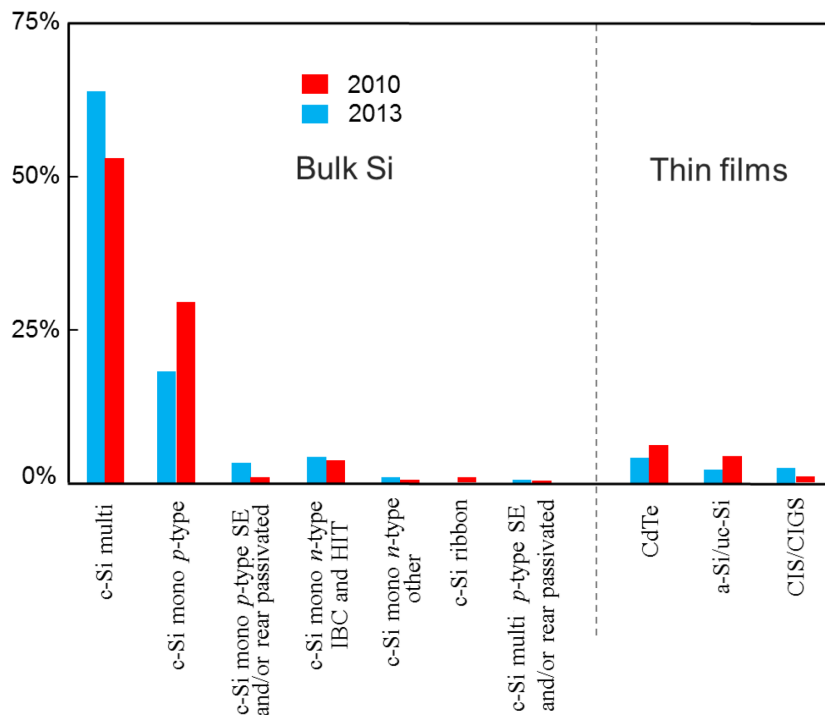


Figure 1. Market share of competing photovoltaics technologies in 2010 and 2013. Ref. [3].

have recently risen from 10.7% [6] to 16.1% [7] and CIGS panels improved their performance from 13.4% [8] to 15.7% [9]. However, only incremental efficiency improvement from 10.4% [10] to 10.9% [11] has been achieved for Si thin-film panels over a period of more than 15 years, although theory predicts 15% or even higher for micromorph double-junction a-Si:H/ μ c-Si:H solar cells and 17% for triple-junction a-Si:H/a-SiGe:H/ μ c-Si:H devices [12].

In this article, following a brief discussion of factors limiting the performance of semiconductor solar cells, we discuss thin-film silicon solar cells, which include single junction a-Si:H and microcrystalline cells as well as multijunction a-Si:H and a-Si:H/ μ c-Si:H, the latter also known as micromorph Si cells. We focus on the current status of these technologies, major development directions, cost cutting strategies, and outstanding challenges in the light of their economic viability.

2. Power conversion efficiency of semiconductor solar cells

In a nutshell, semiconductor solar cells are $p-n$ (or $p-i-n$) photodiode structures that convert incident light directly into electricity (photovoltaic effect). A detailed discussion of solar cell operation principles is readily available in the literature (e.g., see [13]) and only a succinct discussion is given here for convenience. Photons with energies greater than the bandgap of the semiconductor used are absorbed, which generate electron-hole pairs. The electron-hole pairs generated within the depletion region of the $p-n$ or $p-i-n$ junction and within a region of minority-carrier diffusion length from the edge of depletion region are transported in opposite directions by the electric field of the depletion region to an external load. The conversion efficiency of light to electric power, η , for a solar cell can be expressed as follows:

$$\eta = I_{sc}V_{oc}EF/P. \quad (1)$$

Here I_{sc} is the short circuit current, V_{oc} is the open circuit voltage, FF is the fill factor (defined as the ratio of the actual maximum power generated by the cell divided to the theoretical limit power defined as $(I_{sc}V_{oc})$ (or the area under the I-V curve in the fourth quadrant divided by $I_{sc}V_{oc}$)), and P is the incident-light power. The major parameters determining the efficiency of a solar cell are illustrated in Figure 2 (shaded area shows the maximum power generated by the solar cell). Since the actual illumination conditions vary widely with geographical location, season, day time, and weather conditions, for standardization purposes, the power conversion efficiency of solar cells produced by different companies and research laboratories is measured under standard illumination with simulated air mass (AM) spectra. For thickness A_0 of the earth atmosphere, the path length of the solar light through the atmosphere is equal to

$$A = A_0/\cos\theta \quad (2)$$

where θ is the angle between the elevation of the sun and the azimuth. AM0 and AM1.5 are used to test solar cells for space and terrestrial applications, respectively. The AM0 spectrum represents the solar spectrum outside the earth's atmosphere, where zero means "zero atmosphere". The AM1.5 spectrum simulates the sun illumination on the earth's surface at mid-latitudes for the air mass coefficient $1/\cos\theta = 1.5$ (or $\theta = 48.2^\circ$). For the case of the AM0 and AM1.5 spectra, the power of incident light is 1367 Wm^{-2} and 963 Wm^{-2} , respectively. Reference spectra, tabulated in the American Society for Testing Materials Standard ASTM E891-87 (direct normal) and ASTM E892-87 (global), provide the basis for the other national and international standards.

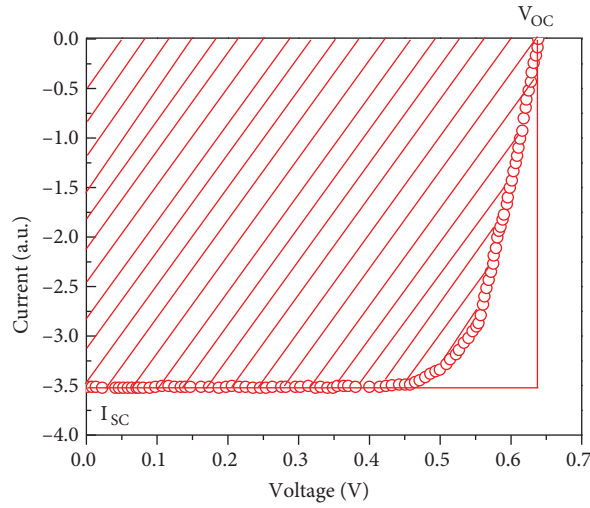


Figure 2. Output characteristic of a representative bulk Si solar cell.

Let us consider factors limiting the power conversion efficiency of solar cells based on Eq. (1). The short circuit current generated by an ideal solar cell is equal to

$$I_{SC} = egS(w + L_n + L_p), \quad (3)$$

where e is the elementary charge, g is the carrier generation rate expressed as the number of electron-hole pairs generated per unit volume per second, S is the light absorbing surface area of the PV device, w is the width of the depletion region, and L_n and L_p are the diffusion lengths of minority carriers on the p and n sides of a p-n junction, respectively. For a given g value, the I_{SC} value increases with decreasing bandgap of the light-absorbing semiconductor, because a larger portion of the solar spectrum is absorbed (imbedded in g). The I_{SC} value is also proportional to the generation volume equal to $S(w + L_n + L_p)$. This volume increases with a decrease in doping level on each side of the device because w , L_n , and L_p all increase. However, the decrease in doping below some concentration may degrade the device efficiency drastically because of a substantial increase in the series resistance. Therefore, a trade-off must be reached for optimum performance. In commercial solar cells, the width of the depletion regions is usually no more than a few microns.

The other important parameter determining the power is the open circuit voltage, V_{OC} . This parameter in an ideal solar cell increases with increasing bandgap of the semiconductor used as the light absorbing material, because

$$V_{OC} = (kT/e) \ln(I_{SC}/I_0), \quad (4)$$

where $I_0 \sim \exp(-E_g/kT)$ is the reverse saturation current.

The caveat is that the fill factor FF of a solar cell, determined as the area formed by the IV relationship in the fourth quadrant of the p-n junction normalized to the product of the open circuit voltage and short circuit current, decreases rapidly with increasing series resistance. As an example, a series resistance of only 5 Ω reduces the SC power conversion efficiency by more than 70% compared to the case of zero series resistance [14].

The series resistance is mainly composed of the bulk resistances of the n- and p-type sides of the solar cell and the contact resistances. The increase in the doping concentration of n and p regions reduces both the semiconductor resistance and specific contact resistances. However, as mentioned above, an increase in

the doping level reduces the generation volume and, therefore, I_{SC} . Therefore, a trade-off is required between increasing FF and decreasing I_{SC} . In a similar manner, V_{OC} increases with increasing semiconductor bandgap, while I_{SC} decreases. Because the power conversion efficiency is governed by the product ($I_{SC}V_{OC}$), the maximum efficiency is reached for an optimum energy bandgap. The power conversion efficiency as a function of a semiconductor bandgap, which has been calculated for black-body limit and AM1.5 and AM0 spectra [15], is shown in Figure 3. For terrestrial electrical power generation from unconcentrated light (AM1.5 spectrum), the optimum bandgap is 1.34 eV, which is close to the bandgaps of CdTe, InP, GaAs, and CuInS₂ [13,16,17].

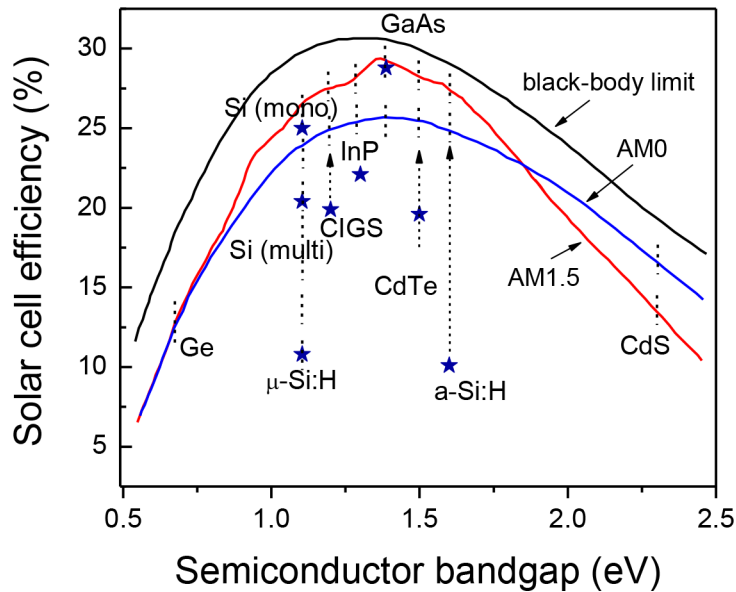


Figure 3. Power conversion efficiency of single-junction solar cells as a function of semiconductor band gap. Asterisks show the best confirmed solar cells efficiencies under AM1.5 illumination (after Ref. [15]).

The power conversion efficiency of a single-junction SC is governed by the thermodynamical Shockley–Queisser limit of $\sim 31\%$ for unconcentrated solar light [18]. This means that an ideal PV device operating under direct sunlight would at best convert approximately 30% of the solar radiation into electrical power, but worse in reality as the actual cells suffer from parasitic losses. In addition to the series resistance mentioned above, charge carrier recombination at grain boundaries, surfaces, interfaces, and defects also decreases the efficiency of SCs. Semiconductors with energy bandgaps ranging from 1.0 to 1.7 eV are used for manufacturing PV modules in practice [19]. This variety includes but is not limited to monocrystalline, multicrystalline, and microcrystalline silicon ($E_g = 1.12$ eV), Cu(In,Ga)Se₂ ($E_g \sim 1.3$ eV), GaAs ($E_g = 1.4$ eV) and related materials, CdTe ($E_g = 1.5$ eV), and hydrogenated amorphous silicon ($E_g = 1.7$ eV).

3. General characteristics of thin-film solar cells

As alluded to above, thin-film solar cells are usually referred to as second generation photovoltaics. These devices share the same performance restrictions as those laid out by the Shockley–Queisser treatment as the bulk-Si photovoltaics. The lure is the promise to substantially lower the production cost [20], because they do not require the use of semiconductor wafer substrates and their fabrication technologies utilize lower process temperatures.

Thin-film Si solar cells (amorphous, microcrystalline, and their combinations) share many common features with other thin-film PV technologies (CdTe and CIS/CIGS):

(i) Devices are fabricated on foreign substrates (glass, metal, flexible polymers).

(ii) Transparent conducting oxide (TCO) layers are generally used for the front contact, whereas a reflective contact material (silver, Ag, frequently in combination with a TCO interlayer for better refractive index matching) is employed on the back surface to enhance light trapping within absorber layers. The optical quality of these materials is a critical factor determining the required thickness of the absorber layers in terms of ensuring the absorption of an optimum amount of light.

(iii) Depending on the application, solar cells can be fabricated in either a “substrate” or a “superstrate” configuration (Figure 4). In the case of the superstrate configuration, the layers are deposited in a reverse sequence, from the top (front) to the bottom (back) on TCO-coated transparent glass substrates. The deposition begins with a contact window layer of a photodiode and is finished by a back reflector on top. Light enters the cell through the glass substrate. An important requirement for the TCO as a substrate material, in addition to high electrical conductivity and optically transparency, is the chemical stability in the process environment during solar-cell material deposition. The superstrate configuration is particularly suited for building-integrated solar panels to a glass substrate, which would also function as an architectural element.

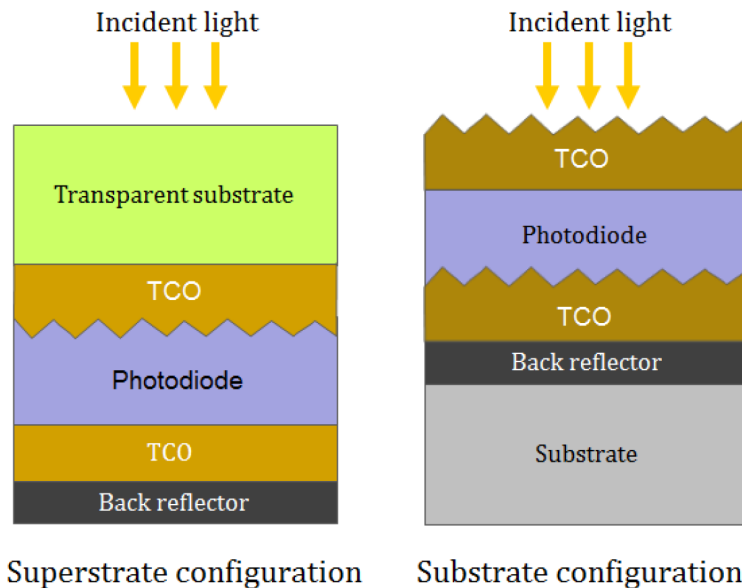


Figure 4. Schematics of thin-film solar cells fabricated in “superstrate” (left) and “substrate” (right) configurations.

The substrate configuration requires the fabrication of solar cells from the back to the front. The deposition begins from the back reflector and ends with a TCO layer. For many special applications, the use of lightweight and unbreakable substrates, which include stainless steel, polyimide, or polyethylene terephthalate (PET), is advantageous. These substrates can be either opaque, as in the case of stainless steel or transparent, as in the case of PET. The latter ones are often easily damaged by ultraviolet light, as most plastics. It should be noted that the plastic substrates generally limit the process temperatures to approximately 150 °C, which makes them suitable only for manufacturing of a-Si modules.

In contrast to the very mature bulk-Si PV devices, which are already very close to the theoretical limit of efficiency, thin-film photovoltaics are well below their potential. Although, as discussed in the Introduction

section, substantial progress has been made in recent years in CdTe and CIGS PV modules, these thin-film technologies are in the nascent manufacturing stage, and performance of small-area laboratory cells will not necessarily translate to large modules when manufacturing of such is attempted.

4. Amorphous silicon

Hydrogenated amorphous silicon (a-Si:H) is a quasidirect bandgap material with E_g of 1.7–1.8 eV that gives rise to a large absorption coefficient of $>10^5 \text{ cm}^{-1}$ for photons with energies greater than the bandgap. This permits much thinner absorbing layers to be used, which translates to lower materials cost compared to crystalline silicon. The presence of hydrogen is critical for passivating the dangling bonds and other defects associated with random arrangement of silicon atoms. Essentially this material can be construed as a solid solution of Si and hydrogen.

Besides PV modules, a-Si is widely employed in color sensors and scanners and thin-film transistors for flat panel displays. All the above-mentioned applications take advantage of the great versatility of this material, which is deposited at low temperatures (150 to 350 °C) using a variety of high-throughput techniques, most of them being originally developed for the mainstream Si industry. Because of short minority-carrier lifetimes in a-Si:H, especially in the doped varieties, efficient collection of photogenerated carriers requires the assistance of an electric field. Therefore, the $p-i-n$ photodiode configuration is employed for a-Si:H solar cells with the intrinsic layer acting as a light absorber where there is a built-in electric field. Because of the inferior quality of doped a-Si:H, thin layers ($<100 \text{ nm}$) of doped microcrystalline Si are usually employed as p - and n -contacts ($\mu\text{c-Si}$ will be discussed in more detail in the next section). The a-Si:H optical bandgap of 1.7–1.8 eV is wider than that of crystalline silicon (1.1 eV). As a result, a-Si:H solar cells exhibit higher open-circuit voltages; however, the photocurrent is limited by absorption of a smaller portion of the solar spectrum. In multijunction SCs, which will be discussed below, alloying of Si with Ge and carbon allows one to obtain a material with narrower and wider energy bandgap, respectively. The first solar cells based on a-Si:H were reported in 1976 by Carlson and Wronski [21]. The a-Si:H SCs are the first commercially successful thin-film PV technology [22]. Although this technology still has an important position in consumer electronics, the number of companies producing a-Si PV modules has been falling over time.

Schematic of a $p-i-n$ single-junction a-Si solar cell developed by the Kaneka Company is shown in Figure 5 [23]. The efficiency of this device is close to 7% [23]. The cell is fabricated in superstrate configuration. The a-Si:H absorbing layer is deposited on a TCO film serving as a front electrode. The front TCO should exhibit a low sheet resistance (no more than $\sim 10 \text{ } \Omega/\text{sq}$) and high optical transmission (no less than 85%, preferably above 90%) in the range from near UV to near IR (details on TCO materials for photovoltaics with specific data on conductivity and optical transmittance can be found elsewhere [24]). The surface of the TCO layer is textured in order to improve light trapping. A double-layer stack consisting of ZnO:Al and Ag films acts as a back surface reflector [23,25].

Unfortunately, the efficiency of a-Si solar cells working under light exposure degrades with time due to the Staebler–Wronski effect [26], which is directly related to formation of defects (dangling bonds, microvoids, stressed regions) acting as recombination centers [27]. The exact mechanism of this phenomenon is still an issue of current debate [28]. As a result, the efficiency of commercial modules exposed to sunlight drops to 5%–6% over a period of months despite the initial efficiencies exceeding 12% for laboratory a-Si cells. Thus, the greatest challenge facing the a-Si technology remains the maintaining of the initial efficiency. During the last 2 decades, a great deal of effort has been devoted to mitigate this problem, albeit with limited success. One of the

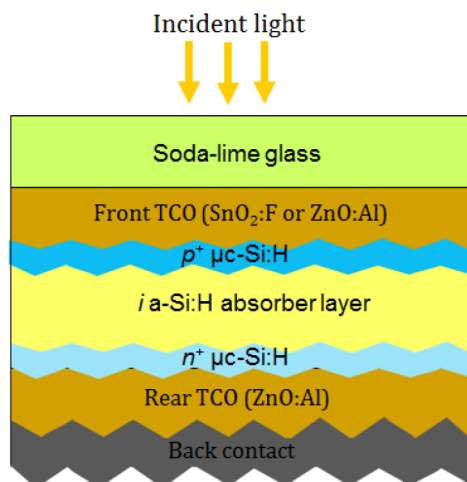


Figure 5. Schematic of a state-of-the-art p-i-n a-Si:H solar cell fabricated on a TCO-coated glass superstrate (after Ref. [23]).

possible solutions to the light-induced degradation of a-Si solar cells is reducing the amorphous layer thickness. This reduces the distance that photogenerated carriers must traverse before they reach the electrodes and thus minimize recombination losses. However, this comes at the expense of reduced light absorption in the cell. The effective layer thickness and, therefore, absorption can be increased with the use of optical confinement techniques employing front and back reflectors. Another approach to limit the light-induced degradation of solar cells is optimizing growth conditions in order to achieve the microstructure close to the amorphous-to-microcrystalline transition region (more details on this topic can be found in a review article by Schroopp et al. [29]). To date, the highest stable efficiency of 10.1% for a small-area single-junction a-Si:H cell has been reported by Benagli et al. [30]. The stable efficiency for large commercial state-of-art single-junction modules does not exceed 7% [31]. In recent years, the material quality, manufacturing techniques, and design of single-junction a-Si:H cells have progressed to the stage where very little room appears to be left for further improvement of their efficiency.

Another approach for improving the stabilized efficiency of a-Si:H SCs that has been adopted by the majority of manufacturers is the use of a stack of 2 or 3 cells (tandem or triple junction design), as illustrated schematically in Figure 6 [32]. The chief advantage of this design is more efficient absorption of the solar spectrum by forming a composite absorbing layer featuring multiple bandgaps. This approach also allows the use of thinner layers to absorb the same or even larger number of photons, thus mitigating the light-induced efficiency degradation. In addition, the collection of photogenerated carriers is improved because the thinner absorbing layers give rise to larger electric fields. The multijunction design is particularly successful for amorphous materials because there is no need for lattice matching, which is required for crystalline heterojunctions. The relatively low substrate temperature used for a-Si deposition has the benefit that the underlying layers are not affected during subsequent deposition steps. The fabrication cost of multiple $p-i-n$ structures is higher (but not substantially) due to increased deposition time of the multilayer stacks.

Figure 6a shows a schematic sketch of a triple-junction a:Si:H/a-SiGe:H/a-SiGe:H solar cell. The top layer, made of a wide-bandgap material, absorbs high-energy photons and passes the photons with energies lower than its bandgap, which generate electron-hole pairs in the lower absorber layers with narrower bandgaps. The cells in the stack are connected by electrically tunnel junctions. Amorphous Si:H with a relatively high

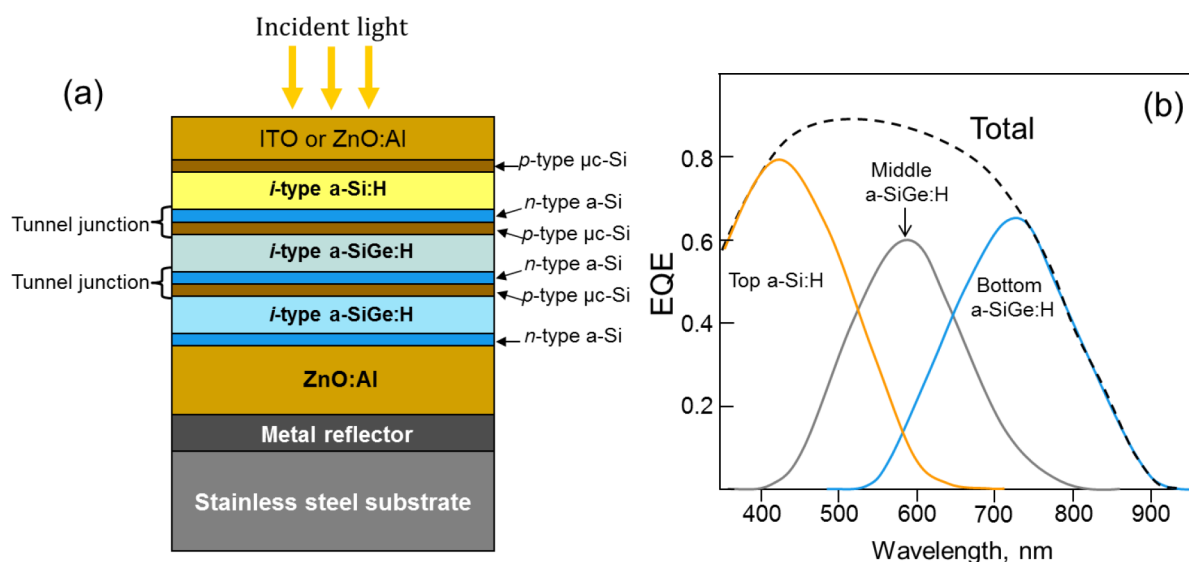


Figure 6. (a) Cross section schematic of a spectrum-splitting, triple-junction a-Si:H/a-SiGe:H/a-SiGe:H solar cell and its (b) stabilized external quantum efficiency (after Ref. [32]).

concentration of hydrogen is commonly used as the wide bandgap (1.8 eV) material for the top absorbing layers in multijunction cells [33]. Although alloying of Si with carbon (a-SiC:H) allows increasing of the bandgap up to 2.2 eV [34], a-SiC:H degrades substantially upon light soaking (exposing to light for some period) and, therefore, the a-SiC:H layers should be very thin, which reduces light absorption in the cell and thus the generated current. The bottom absorber layers in the multijunction solar cells are usually made of a-SiGe:H [35]. Depending on the Ge content, the bandgap of a-SiGe:H can be adjusted from 1.7 to 1.1 eV. For the maximum efficiency of a tandem a-Si:H/a-SiGe:H solar cell a bandgap of about 1.2 eV is desirable [36]. However, the optoelectronic properties of a-SiGe:H deteriorate progressively and considerably with increasing Ge concentration, and only a-SiGe alloys with a bandgap of no less than 1.4 eV are practical. Thus, the absorber layers of middle and bottom cells are typically made of a-SiGe:H with bandgaps of 1.6 eV and 1.4 eV, respectively [33]. The a-Si:H/a-SiGe:H and a-Si:H/a-SiGe:H/a-SiGe:H (with bandgaps of 1.8, 1.6, 1.4 eV) designs of tandem and triple-junction cells, respectively, are the most popular. a-Si:H/a-SiGe:H (1.8, 1.4 eV) and a-Si:H/a-SiGe:H/a-SiGe:H (1.8, 1.7, 1.4 eV) cells are also produced but with lower efficiencies because of the less optimum combination of bandgaps.

Because the current must be the same through all the cells in the triple-junction stack, the thickness of each absorber layer should be tuned to achieve current matching with the top absorber layer limiting the current. The fill factor is the lowest for the bottom a-SiGe:H and the highest for the top a-Si:H cell in the triple-junction a-Si:H/a-SiGe:H/a-SiGe:H cells because the bandgap decreases from the top to the bottom absorber. Therefore, the value of J_{SC} should be the highest for the bottom cell, lowest for the top cell, and intermediate for the middle cell, with the optimal difference in about 1 mA/cm². This is usually dubbed as an intentional “mismatch” in the J_{SC} values designed to match the cells at the operating point. To improve collection of photogenerated holes and thus the FF value in a-SiGe:H-based multijunction cells, bandgap grading with the lowest-gap material located near the *i/p* interface can be used [37,38]. Optimized small-area triple-junction cells show a stabilized efficiency of about 13% [33]. The stabilized efficiency of double- and triple-junction modules is >9.5% and >10%, respectively [39].

Nowadays, the fabrication technology of a-Si:H cells is relatively well-established. For a-Si:H thin film deposition, modified vapor phase deposition (CVD) techniques are commonly used. Among them are plasma-enhanced CVD (PECVD) [40,41] and hot-wire CVD (HWCVD) [42]. Both methods utilize silane (SiH_4) and hydrogen-containing gas mixtures. The HWCVD technique, relying on thermal dissociation of SiH_4 on hot (>1500 °C) metal (tungsten or tantalum) wires, has the advantages of higher deposition rates (of the order of 10 nm/s for high quality material [43] vs. 0.1–0.5 nm/s for PECVD), better uniformity, and absence of dust and ion damage. In addition, the substrate is not an integral part of the deposition mechanism in the HWCVD process, which makes a wider selection of substrates possible. Insulating and conducting, rigid and flexible substrates, such as thin metallic sheets and plastics, may be used. The addition of dopant gases into the gas mixture allows doping of growing films. Due to the possibility of almost completely depleting the source gases, the HWCVD technique provides also a high degree of utilization of the process gases up to 80% [44], whereas the typical value of gas utilization is around 10% for a-Si:H solar cell production and can be as low as 1% for TFT display production (see, for example, a detail review of the HWCVD technique in the context of solar cell production [45]). The main weakness of this method is that growing films are exposed to thermal radiation from the hot wires, which makes substrate temperature control very challenging. Another challenge with commercial cells is the fabrication of spatially uniform a-Si:H and TCO over a large area (of the order of square meters) [46].

The a-Si:H cell technology benefits from the development of large-scale, high-throughput PECVD deposition systems used for fabrication of liquid crystal displays (LCDs). Several manufacturers of LCD processing equipment also offer turn-key production lines for a-Si:H PV modules. Various PECVD configurations (batch-type, cluster tool, inline) are available. For 1.4 m² glass size, modern PECVD systems have a throughput of well over 10 MWp/year based on single-junction a-Si:H PV modules [23]. Recently, Applied Materials has introduced the equipment for 5.7-m² solar panels and started to sell their turn-key lines to manufacturers [47]. The next attractive size is 9.0 m², which is currently at the introduction stage for TFT-LCD displays (investments by Sharp, Samsung, Sony, and LG). Owing to the continuous development of manufacturing techniques, further cost reduction can be expected, while considerable efficiency improvement poses a great challenge.

5. Microcrystalline Si and “micromorph” solar cells

Microcrystalline silicon ($\mu\text{c-Si}$) can be used not only for high conductivity *p*- and *n*-contacts, but also as a material for active layers in thin-film solar cells. The possibility to use $\mu\text{c-Si}$ for the fabrication of photosensitive layers was demonstrated in the early 1990s [48,49], and the first $\mu\text{c-Si:H}$ solar cells showing reasonable efficiency of 4.6% were fabricated in 1994 [50]. The bandgap of $\mu\text{c-Si:H}$ is close to that of crystalline Si, which allows extension of the absorption range to red and infrared light. Hydrogen passivation suppresses carrier recombination at grain boundaries, thus improving device performance. Most importantly, $\mu\text{c-Si}$ solar cells are less subject to light-induced degradation and show better stabilized efficiencies as compared to those attainable from a-Si:H devices.

Thin films of $\mu\text{c-Si:H}$ are deposited by PECVD techniques with very high hydrogen concentration at substrate temperatures of around 200 °C. This material is actually a mixture of crystalline and amorphous phases, and the material properties depend strongly on the preparation conditions, especially silane-to-hydrogen ratio in the process gas mixture [51]. As demonstrated by Vetterl et al. [51], $\mu\text{c-Si:H}$ with the properties best suited for solar cell applications (combination of highest FF, highest J_{SC} , and highest V_{OC}) are obtained

under deposition conditions close to the amorphous-to-microcrystalline transition point. With this approach, single-junction cells with stabilized efficiencies exceeding 10% (typical values $V_{OC} = 0.52$ V, FF = 0.74) have been achieved [52]. So far, the highest independently confirmed value of conversion efficiency of 10.8% is for small-area devices reported by Sai et al. [53].

The major disadvantage of μc -Si is that its absorption coefficient is lower than that of amorphous material [54]; therefore, thicker layers of μc -Si (1–2 μm) are required for efficient light absorption. In addition, the deposition rate for μc -Si films is much lower (few nm/min) as compared to that for a-Si (10–30 nm/min), which increases the cost of μc -Si-based cells. As a result, the PV modules based on single-junction μc -Si:H cells do not seem to be commercially viable at present. Therefore, considerable effort is exerted on developing deposition techniques capable of providing higher rates without degrading the power conversion efficiency. Various modifications of the widely used PECVD method have been proposed, including very high frequency (VHF) PECVD utilizing frequencies of 40 to 60 MHz [50,55,56], high-pressure PECVD [57–59], and the combinations thereof [60–62]. The HWCVD technique [45,63] has also received much attention due to its high growth rate, highly efficient process gas utilization, and large area capability [64].

Low deposition rates together with the high capital equipment cost, needed for deposition of thick μc -Si:H layers, limit the market penetration of the μc -Si:H technology; however, μc -Si:H may be used as narrow-bandgap material in tandem cells. The combination of μc -Si:H with 1.1-eV bandgap and a-Si:H 1.7-to-1.8-eV bandgap in double or triple junction solar cells (in the latter case a SiGe layer a bandgap of ~ 1.4 to 1.5 eV is usually used as an intermediate absorber between μc -Si:H and a-Si:H) improves the power conversion efficiency substantially owing to more optimum use of the solar spectrum (Figures 7 and 8). This in turn reduces the cost of power generation [65]. The production cost can potentially be reduced to 0.35 €/Wp [66]. Meir et al. [67] coined the term “micromorph” cells for these tandem devices. Replacing a-SiGe with μc -Si in the a-Si:H/a-SiGe:H tandem solar cells reduces the materials cost due to the use of SiH_4 instead of the more expensive GeH_4 . Other advantages of the micromorph cells over multijunction a-Si:H cells with a-SiGe:H layers are the negligible light-induced degradation and higher values of FF and quantum efficiency in the long wavelength region. The downside is the need for thicker (as compared to a-SiGe:H) absorbing layers and lower V_{OC} of μc -Si:H solar cells as compared to that of a-SiGe cells (0.53 V vs. > 0.6 V). Further increase in the deposition rate of μc -Si:H and improvement of light-trapping schemes would alleviate some if not all the above-mentioned problems.

A schematic view of a micromorph solar cell is shown in Figure 7a. In the multijunction amorphous/microcrystalline Si solar cells, the top a-Si:H absorber layer is made as thin as possible (typically 0.2–0.3 μm) to minimize the light-induced efficiency degradation. The intermediate reflector (IR) placed between the a-Si:H and μc -Si:H cells (see Figure 7a) reflects the light back into the top cell and thus allows reduction of the thickness of the a-Si:H absorber layer without compromising the short-circuit current of the top cell, which sets the current through the entire tandem device [68–70]. Additionally, the IR further improves current matching in tandem cells by reducing the short-circuit current of the bottom cell, which is typically excessive and thus partially wasted. The IR is made of a material with a lower refractive index ($n \sim 1.5$ –2.2) compared to the a-Si:H ($n \sim 4$) and μc -Si:H absorbers ($n \sim 3.4$). The IR layer obviously should be as conductive as possible, the latter for minimizing electrical losses. ZnO was initially used as a material for the intermediate reflectors [71,72]. Unfortunately, ZnO reflectors should be deposited ex situ and their use in large modules would result in additional laser scribe for monolithic series interconnection to avoid lateral shunting of the segments. Nanostructured hydrogenated silicon oxide (nc-SiOx:H) allowing in situ deposition was found to be a more suitable

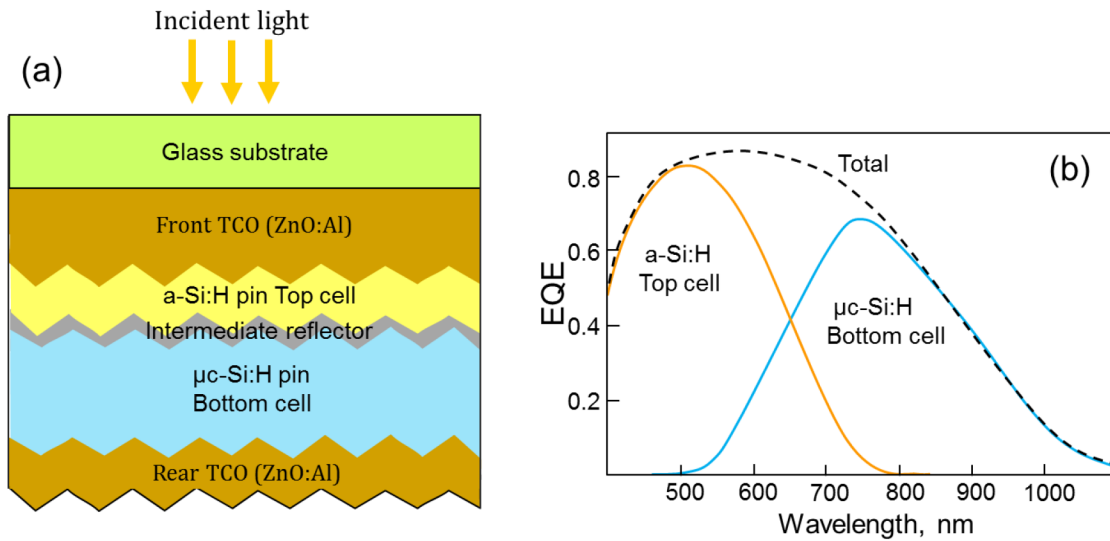


Figure 7. (a) Schematic structure of a tandem a-Si:H/ μ c-Si:H solar cell with front and back ZnO:Al contact layers grown by low-pressure CVD and with an intermediate reflector to enhance the top cell current and (b) its stabilized external quantum efficiency (after Ref. [72]).

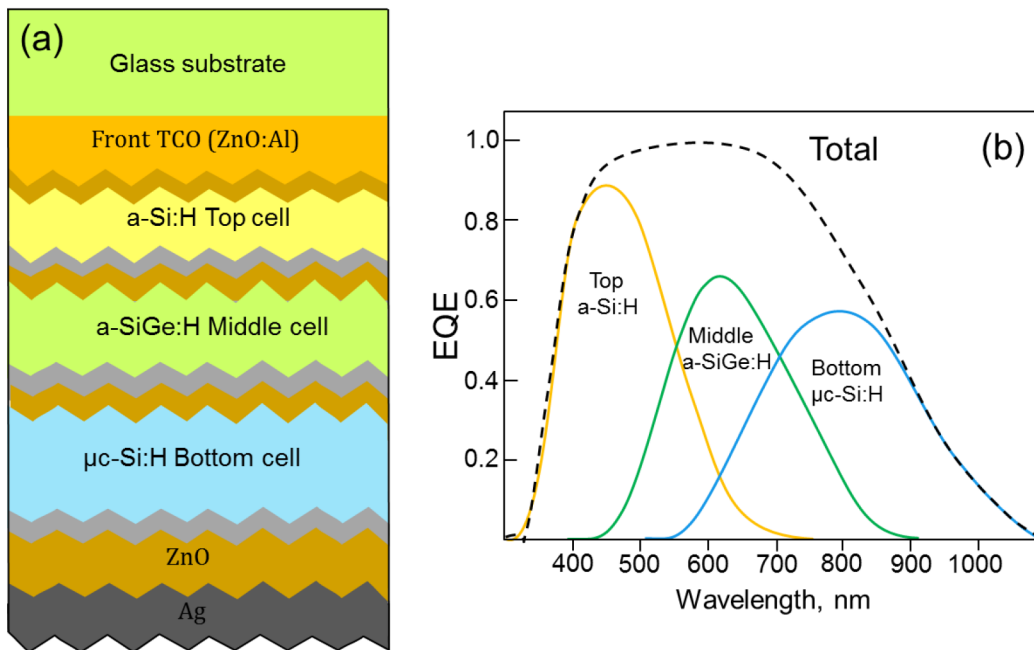


Figure 8. (a) Schematic structure of a triple-junction a-Si:H/a-SiGe:H/ μ c-Si:H solar cell and (b) its stabilized external quantum efficiency (after Ref. [87]).

material for intermediate reflectors [73]. Moreover, scattering of blue-green light absorbing in the top cell can be further enhanced by roughening of the IR top surface with a typical feature size of around 300 nm, while keeping soft or U shape morphology with feature size of 1 μ m for the bottom μ c-Si:H cell. This approach has been termed asymmetric IR [74].

Further improvement of the micromorph cell performance can be achieved with the use of the intermediate

a-SiGe:H ($E_g \sim 1.5$ eV) absorber layer. Figure 8 shows the schematic of the triple junction a-Si:H/a-SiGe:H/ μ c-Si:H solar cell. Theoretical performance of the triple-junction cell is estimated at 17%. This implies that further optimization of light-trapping approaches and contacts [12] is required. Accordingly, the major efforts to increase power conversion efficiency of thin-film Si solar cells are mainly focused on exploration of new concepts for better light trapping and improved contacts. In line with the former direction, employment of 1D and 2D photonic crystals as surface antireflection intermediate reflectors for improved broadband angular light acceptance [75,76], distributed Bragg reflectors [77], and plasmonic nanostructure gratings [78–82] as intermediate and back reflectors are the major research directions. Novel approaches to contact materials aim to improve contact transparency for incident light through enhancement of optical bandgap energy and adjustments of refractive index over a considerable wavelength range while keeping high electrical conductivity. For this application, microcrystalline silicon oxide (μ c-SiO_x:H) alloys prepared by PECVD are considered a promising material class owing to their wide bandgap and the possibility to achieve both n- and p-type conduction via doping [69,70,83–85]. This material makes use of the high electrical conductivity of doped μ c-Si:H and the high optical transparency of amorphous silicon oxide [73,86]. A small fraction of highly conductive μ c-Si:H embedded into the wide-bandgap a-SiO_x:H layer provides sufficiently low resistivity (less than $10^{-5}\Omega$ cm). Due to a very low refractive index, n-type μ c-SiO_x:H can be used as intermediate and back optical reflector, and p-type μ c-SiO_x:H can serve as a window layer owing to its wide bandgap. With this approach, an initial efficiency of 16.1% (in-house measurement) for the a-Si:H/a-SiGe:H/ μ c-Si:H stack and a stabilized efficiency of 13.4% (confirmed by NREL) for the a-Si:H/ μ c-Si:H/ μ c-Si:H stack have been recently achieved for small-area (1 cm × 1 cm) triple-junction solar cells [87]. Another material family showing promise as the top highly conductive window is microcrystalline hydrogenated silicon carbide (μ c-SiC:H), which is naturally n-type [88]. In addition, novel doping layers, such as n-type microcrystalline silicon oxide (μ c-SiO_x:H), which has a very low refractive index, and p-type microcrystalline silicon oxide (μ c-SiO_x:H), which has a wide bandgap, were successfully used as an optical reflector and the window layer, respectively.

Owing to more efficient use of the solar spectrum, translating into higher power conversion efficiencies and better stability, the micromorph solar cells appear to be a better option compared to the devices entirely based on a-Si:H. Already the micromorph concept has been adopted by many companies producing commercial PV modules. For instance, Kaneka, one of the leaders in a-Si:H solar cells, offers a wide range of products from rooftop to semitransparent designs for building integration [89]. It offers 110-Wp modules with the dimensions of 1210 × 1008 mm, with an associated stabilized module efficiency exceeding 10% [90]. Several other companies have also announced the manufacture of micromorph PV modules. Recently, such “big” players as Sharp and LG have started development and production of micromorph Si solar cells. The best efficiency of 10.9% for large modules based on triple-junction a-Si:H/a-SiGe:H/ μ c-Si:H cells has been achieved recently by LG Electronics [91].

6. Conclusion

In this article, we overview thin-film Si solar photovoltaics, encompassing amorphous, microcrystalline, and micromorph solar cells. The a-Si:H solar cells represent one of the first commercially sustainable photovoltaic technologies and the oldest thin-film technology in the market with a strong position in consumer electronics. However, today this technology faces very tough competition from other thin-film technologies and the bulk-Si variety that have substantially reduced cost through an aggressive and very efficient cost-cutting effort. The major problem associated with the a-Si:H solar cells is the relatively low power conversion efficiency. After

many years of research, only limited success has been achieved in mitigating light-induced degradation, which undermines the stabilized efficiencies of a-Si:H solar cells. The gap between the efficiency of the best triple-junction commercial a-Si modules and the small-area laboratory devices is marginal (10% vs. 13%). What is more concerning is that virtually no efficiency improvement has been demonstrated of late. Therefore, further reductions in the \$/Wp cost of energy generated by a-Si:H modules can be expected only from development of more cost-efficient manufacturing techniques and larger scale production. The cost-cutting efforts made it possible to keep the price per Wp power for a-Si:H solar cells among the lowest in the industry (currently approaching \$ 0.5/Wp for the new generations of PV modules). However, it may become insufficient in the near future.

Micromorph solar cells represent a relatively young technology that has just entered the market place. They show the greatest promise among Si-based thin-film solar cells currently on the market. The highest efficiencies of around 11% for micromorph modules have already exceeded the values achieved for the best a-Si:H multijunction solar cells and have the potential to reach 15%. Further improvement in their performance is expected through the development of better, more efficient light-trapping schemes and developing highly conductive and transparent contacts.

References

- [1] <http://www.solarbuzz.com/news/recent-findings/record-breaking-demand-global-solar-pv-industry-according-npd-solarbuzz>.
- [2] <http://www.solarbuzz.com/news/recent-findings/solar-pv-industry-targets-100-gw-annual-deployment-2018-according-npd-solarbuzz>.
- [3] <http://www.solarbuzz.com/resources/articles-and-presentations/pv-technology-change-before-2015>.
- [4] <http://www.forbes.com/sites/greatspeculations/2013/12/23/first-solar-regaining-its-edge-over-chinese-manufacturers/>.
- [5] <http://www.solar-facts-and-advice.com/micromorph.html>.
- [6] Cunningham, D.; Davies, K.; Grammond, L.; Mopas, E.; O'Connor, N.; Rubcich, M.; Sadeghi, M.; Skinner, D.; Trumbly, T. In *Conference Record; 28th IEEE Photovoltaic Specialists Conference*, Alaska, September, 2000, p. 13.
- [7] First Solar Press Releases, February 26 and April 9, 2013.
- [8] Tanaka, Y.; Akema, N.; Morishita, T.; Okumura, D.; Kushiya, K. In *Conference Proceedings; 17th EC Photovoltaic Solar Energy Conference, Munich, October, 2001*, p. 989.
- [9] <http://www.miasole.com>.
- [10] Yang, J.; Banerjee, A.; Glatfelter, T.; Hoffman, K.; Xu, X.; Guha, S. In *Conference Record, 1st World Conference on Photovoltaic Energy Conversion*, Hawaii, December, 1994, p. 380.
- [11] Ahn, S. W.; Lee, S. E.; Lee, H. M. In *Conference Proceedings: 27th European Photovoltaic Solar Energy Conference*, Frankfurt, September 2012, p. 3AO5.1.
- [12] Zeman, M.; Krc, J. *J. Mater. Res.* **2008**, *23*, 889.
- [13] Green, M. A. *Solar Cells: Operating Principles, Technology and Systems Applications*; Prentice Hall: Upper Saddle River, NJ, USA, 1992.
- [14] Sze, S. M. *Semiconductor Devices: Physics and Technology*, second ed.; Wiley: New York, NY, USA, 2004.
- [15] Kazmerski, L. L. *J. Electron Spectrosc. Relat. Phenom.* **2006**, *150*, 105–135.
- [16] Loferski, J. J. *J. Appl. Phys.* **27** **1956**, *27*, 777–784.

- [17] Partain L.D. (Ed.), *Solar Cells and Their Applications*, Wiley: New York, NY, USA, 1995.
- [18] Shockley, W.; Queisser H.J., *J. Appl. Phys.* **1961**, *32*, 510-519.
- [19] Miles, R.W.; Zoppi, G.; Forbes, I. *Materials Today* **2007**, *10* 20-27.
- [20] Hamakawa, Y. (Ed), *Thin-Film Solar Cells: Next Generation Photovoltaics and Its Applications*; Springer: Berlin, Germany, 2004.
- [21] Carlson, D. E.; Wronski, C. R. *Appl. Phys. Lett.* **1976**, *28*, 671–673.
- [22] Ginley, D.; Green, M. A.; Collins, R. *MRS Bullet.* **2008**, *33*, 355–364.
- [23] Aberle, A. G. *Thin Solid Films* **2009**, *517*, 4706–4710.
- [24] Liu, H. Y.; Avrutin, V.; Izyumskaya, N.; Özgür, Ü.; Morkoç H. *Superlattices and Microstructures* **2010**, *48*, 458–484.
- [25] Yamamoto, K.; Yoshimi, M.; Tawada, Y.; Fukuda, S.; Sawada, T.; Meguro, T.; Takata, H.; Suezaki, T.; Koi, Y.; Hayashi, K.; et al. *Sol. Energy Mater. Sol. Cells* **2002**, *74*, 449–455.
- [26] Staebler, D.L.; Wronski, C.R. *Appl. Phys. Lett.* **1977**, *31*, 292–294.
- [27] Matsuda, A. *J. Non-Cryst. Solids* **2004**, *338–340*, 1–12.
- [28] Fehr, M.; Schnegg, A.; Rech, B.; Astakhov, O.; Finger, F.; Bittl, R.; Teutloff, C.; Lips, K. *Phys. Rev. Lett.* **2014**, *112*, 066403.
- [29] Schropp, R. E. I.; Carius, R.; Beaucarne, G. *MRS Bullet.* **2007**, *32*, 219–224.
- [30] Benagli, S.; Borrello, D.; Vallat-Sauvain, E.; Meier, J.; Kroll, U.; Hoetzel, J.; Sitznagel, J.; Steinhäuser, J.; Castens, L.; Djeridane, Y. In *Conference Abstracts: 24th European Photovoltaic Solar Energy Conference*, Hamburg, Germany, September 2009.
- [31] Razykov, T. M.; Ferekides, C. S.; Morel, D.; Stefanakos, E.; Ullal, H. S.; Upadhyaya, H. M. *Solar Energy* **2011**, *85*, 1580–1608.
- [32] Wang, W.; Povolny, H.; Du, W.; Liao, X.; Deng, H. In *Conference Record: the 29th Photovoltaics Specialists Conference*, New Orleans, USA, May 2002, p. 1082.
- [33] Yang, J.; Banerjee, A.; Guha, S. *Appl. Phys. Lett.* **1997**, *70*, 2975–2977.
- [34] Hamakawa, Y.; Tawada, Y.; Nishimura, K.; Tsuge K.; Kondo, M.; Fujimoto, K.; Nonomura, S.; Okamoto, H. In *Conference Record; the 16th IEEE Photovoltaic Specialists Conference, Institute of Electrical and Electronics Engineers*, San Diego, CA, USA, September 1982, p 679.
- [35] Yan, B.; Yue, G.; Owens, J. M.; Yang, J.; Guha, S. In *Conference Record: the 2006 IEEE 4th World Conference on Photovoltaic Energy Conversion*, Waikoloa, HI, USA, 2, 2006. p. 1481.
- [36] Takakura, H. *Jpn. J. Appl. Phys.* **1992**, *31*, 2394–2399.
- [37] Guha, S.; Yang, J.; Pawlikiewicz, A.; Glatfelter, T.; Ross, R.; Ovshinsky, S. *Appl. Phys. Lett.* **1989**, *54*, 233–2332.
- [38] Zimmer, J.; Stiebig, H.; Wagner, H. *J. Appl. Phys.* **1998**, *84*, 611–617.
- [39] Green, M. A.; Emery, K.; Hishikawa, Y.; Warta, W. *Prog. Photovolt: Res. Appl.* **2009**, *17*, 85–94.
- [40] Wronski, C. R.; Carlson, D. E. In *Clean Electricity from Photovoltaics*; Archer, M. D.; Hill, R. Eds. Imperial College Press: London, UK, 2001, pp. 199–236.
- [41] Kuwano Y.; Imai, T.; Onishi M.; Nakano, S.; Fukatsu, T. *Jpn. J. Appl. Phys.* **1980**, *19*, 137–141.
- [42] Mahan, A. H.; Carapella, J.; Nelson, B. P.; Crandall, R. S.; Balberg, I. *J. Appl. Phys.* **1991**, *69*, 6728–6730.
- [43] Nelson, B.; Iwaniczko, E.; Mahan, A. H.; Wang, Q.; Xu, Y.; Crandall, R. S.; Branz H. M. In *Extended Abstract: the 1st International Conference on Cat-CVD (Hot-Wire CVD) Process*, 2000, p. 291.
- [44] Ishibashi, K. *Thin Solid Films* **2001**, *395*, 55–60.
- [45] Schroopp, R. I. E. *Thin Solid Films* **2004**, *451–452*, 455–465.

- [46] Lechner P.; Schade, H. *Prog. Photovolt.* **2002**, *10*, 85–97.
- [47] Schroopp, R. E. I. *Jap. J. Appl. Phys.* **2012**, *51*, 03CA07.
- [48] Lucovsky, G.; Wang, C.; Nemanich, R. J.; Williams, M. J. *Sol. Cells* **1991**, *30*, 419–434.
- [49] Faraji, M.; Gokhale, S.; Choudhari, S. M.; Takwale, M. G.; Ghaisas, S. V. *Appl. Phys. Lett.* **1992**, *60*, 3289–3291.
- [50] Meier, J.; Flückiger, R.; Keppner, H.; Shah, A. *Appl. Phys. Lett.* **1994**, *65*, 860–862.
- [51] Vetterl, O.; Finger, F.; Carius, R.; Hapke, P.; Houben, L.; Kluth, O.; Lambertz, A.; Mück, A.; Rech, B.; Wagner, H. *Sol. Energy Mater. Sol. Cells* **2000**, *62*, 97–108.
- [52] Hänni, S.; Alexander, D. T. L.; Ding, L.; Bugnon, G.; Boccard, M.; Battaglia, C.; Cuony, P.; Escarré, J.; Parascandolo, G.; Nicolay, S.; et al. *IEEE Journal of Photovoltaics* **2013**, *3*, 11–16.
- [53] Sai, H.; Saito, K.; Hozuki, K.; Kondo, M. *Appl. Phys. Lett.* **2013**, *102*, 053509.
- [54] Poruba, A.; Fejfar, A.; Remes, Z.; Springer, J.; Vanecek, M.; Kocka, J.; Meier, J.; Torres, P.; Shah, A. *J. Appl. Phys.* **2000**, *88*, 148.
- [55] Vetterl, O.; Finger, F.; Carius, R.; Hapke, P.; Houben, L.; Kluth, O.; Lambertz, A.; Mück, A.; Rech, B.; Wagner, H. *Sol. Energy Mater. Sol. Cells* **2000**, *62*, 97–108.
- [56] Mai, Y.; Klein, S.; Wolff, J.; Lambertz, A.; Geng, X.; Finger, F. In *Conference Proceedings: the 19th EUPVSEC*, Paris, France, 2004, p.1399.
- [57] Roschek, T.; Repmann, T.; Müller, J.; Rech, B.; Wagner, H. *J. Vac. Sci. Technol. A* **2002**, *20*, 492–498.
- [58] Kondo, M.; Matsuda, A. *Curr. Opin. Solid State Mater. Sci.* **2002**, *6*, 445–453.
- [59] Rech, B.; Roschek, T.; Müller, J.; Wieder, S.; Wagner, H. *Sol. Energy Mater. Sol. Cells* **2001**, *66*, 267–273.
- [60] Fukawa, M.; Suzuki, S.; Guo, L.; Kondo, M.; Matsuda, A. *Sol. Energy Mater. Sol. Cells* **2001**, *66*, 217–223.
- [61] Mai, Y.; Klein, S.; Carius, R.; Wolff, J.; Lambertz, A.; Finger, F.; Geng, X. *J. Appl. Phys.* **2005**, *97*, 114913.
- [62] Graf, U.; Meier, J.; Kroll, U.; Bailat, J.; Droz, C.; Vallat-Sauvain, E.; Shah, A. *Thin Solid Films* **2003**, *427*, 37–43.
- [63] Klein, S.; Finger, F.; Carius, R.; Stutzmann, M. *J. Appl. Phys.* **2005**, *98*, 024905.
- [64] Ledermann, A.; Weber, U.; Mukherjee, C.; Schröder, B. *Thin Solid Films* **2001**, *395*, 61–67.
- [65] Shah, A.; Vanecek, M.; Meier, J.; Meillaud, F.; Guillet, J.; Fischer, D.; Droz, C.; Niquille, X.; Fay, S.; Vallat-Sauvain, E.; et al. *J. Non-Cryst. Solid.* **2004**, *338/340*, 639–645.
- [66] Oerlikon Solar. Press release, 16th Jan. 2012.
- [67] Meier, J.; Dubail, S.; Flückiger, R.; Fischer, D.; Keppner, H.; Shah, A. In *Conference Proceedings: the 1st World Conference on Photovoltaic Energy Conversion*, Hawaii, 1994, IEEE, New York, 1994, pp. 409–412.
- [68] Fischer, D.; Dubail, S.; Selvan, J. A. A.; Pellaton Vaucher, N.; Platz, R.; Hof, Ch.; Kroll, U.; Meier, J.; Torres, P.; Keppner, H.; et al. In *Conference Proceedings: the 25th IEEE PVSEC*, Washington, DC, 1996, pp. 1053–1056.
- [69] Yan, B. J.; Yue, G. Z.; Sivec, L.; Yang, J.; Guha, S.; Jiang, C.-S. *Appl. Phys. Lett.* **2011**, *99*, 113512.
- [70] Lambertz, A.; Grundler, T.; Finger, F. *J. Appl. Phys.* **2011**, *109*, 113109.
- [71] Myong, S.Y.; Sriprapha, K.; Miyajima, S.; Konagai, M. *Appl. Phys. Lett.* **2007**, *90*, 263509.
- [72] Meillaud, F.; Feltrin, A.; Domine, D.; Buehlmann, P.; Python, M.; Bugnon, G.; Billet, A.; Parascandolo, G.; Bailat, J.; Fay, S.; et al. *Phil. Mag.* **2009**, *89*, 2599–2621.
- [73] Buehlmann, P.; Bailat, J.; Domine, D.; Billet, A.; Meillaud, F.; Feltrin, A.; Ballif, C. *Appl. Phys. Lett.* **2007**, *91*, 143505.
- [74] Söderström, T.; Haug, F.-J.; Niquille, X.; Terrazzoni, V.; Ballif, C. *Appl. Phys. Lett.* **2009**, *94*, 063501.
- [75] Gomard, G.; Peretti, R.; Drouard, E.; Meng, X. Q.; Seassal, C. *Optics Express* **2013**, *21*, A515–A527.

- [76] Oskooi, A.; Tanaka, Y.; Noda, S. *Appl. Phys. Lett.* **2014**, *104*, 091121.
- [77] Sheng, X.; Liu, J. F.; Coronel, N.; Agarwal, A. M.; Michel, J.; Kimerling, C. L. *IEEE Photonics Technol. Lett.* **2010**, *22*, 1394–1396.
- [78] Paetzold, U. W.; Moulin, E.; Pieters, B. E.; Rau, U.; Carius, R. *J. Photonics for Energy* **2012**, *2*, 027002.
- [79] Paetzold, U. W.; Moulin, E.; Pieters, B. E.; Michaelis, D.; Boettler, W.; Waechter, C.; Hageman, V.; Meier, M.; Carius, R.; Rau, U. *Appl. Phys. Lett.* **2011**, *99*, 181105.
- [80] Moulin, E.; Paetzold, U. W.; Bittkau, K.; Ermes, M.; Ding, L.; Fanni, L.; Nicolay, S.; Kirchoff, J.; Weigand, D.; Bauer, A.; et al. *Mater. Sci. Technol B* **2013**, *178*, 645–650.
- [81] Tan, H. R.; Santbergen, R.; Smetz, A. H. M.; Zeman, M. *Nano Lett.* **2012**, *12*, 4070–4076.
- [82] Moulin, E.; Paetzold, U. W.; Bittkau, K.; Owen, J.; Kirchhoff, J.; Bauer, A.; Carius, R. *Progr. Photovol.* **2013**, *21*, 1236–1247.
- [83] Lambertz, A.; Smirnov, V.; Merdzhanova, T.; Ding, K.; Haas, S.; Jost, G.; Schropp, R. E. I.; Finger, F.; Rau, U. *Sol. Energy Mater. Sol. Cells* **2013**, *119*, 134–143.
- [84] Lambertz A.; Finger, A.; Hollander, B.; Rath, J. K.; Schropp, R. E. I. *J. Non-Crystal. Solids* **2012**, *358*, 1962–1965.
- [85] Yamamoto, K.; Nakajima, A.; Yoshimi, M.; Sawada, T.; Fukuda, S.; Suezaki, T.; Ichikawa, M.; Koi, Y.; Goto, M.; Meguro, T.; et al. *Prog. Photovolt.* **2005**, *13*, 489–494.
- [86] Dominé, D.; Buehlmann, P.; Bailat, J.; Billet, A.; Feltrin, A.; Ballif, C. *Phys. Status Solidi RRL* **2008**, *2*, 163–165.
- [87] Kim, S.; Chung, J.-W.; Lee, H.; Park, J.; Heo, Y.; Lee, H.-M. *Solar Energy Materials & Solar Cells* **2013**, *119*, 26–35.
- [88] Chen, T.; Huang, Y.; Dasgupta, A.; Muysberg M.; Houben, L.; Yang, D.; Carius, R.; Finger F. *Sol. Energy Mater. Sol. Cells* **2012**, *98*, 370–378.
- [89] <http://www.pv.kaneka.co.jp/>.
- [90] http://www.pv.kaneka.co.jp/press_release/091201.html.
- [91] Ahn, S. W.; Lee S. E.; Lee H. M. In Conference Proceedings: *27th European Photovoltaic Solar Energy Conference*, Frankfurt, September 2012. p. 3AO5.1.